

**DESIGN, CONSTRUCTION, AND
TESTING OF THE RETURN
PORTION OF A CLOSED RETURN
WIND TUNNEL**

By

Bernardo J. Langa Jr

A thesis submitted in partial fulfillment of the
requirements for the degree of

Bachelor of Science

Houghton College

September 16, 2020

Signature of Author.....

Department of Physics
September 16, 2020

.....

Dr. Kurt Aikens
Aerodynamics Engineer
Research Supervisor

.....

Dr. Brandon Hoffman
Professor of Physics

**DESIGN, CONSTRUCTION, AND TESTING OF
THE RETURN PORTION OF A CLOSED RETURN
WIND TUNNEL**

By

Bernardo J. Langa Jr

Submitted to the Department of Physics
on September 16, 2020 in partial fulfillment of the
requirement for the degree of
Bachelor of Science

Abstract

A low-speed closed-return wind tunnel is being designed and built at Houghton College. Preliminary efforts focused on choosing the layout and appropriately sizing the tunnel. Once this work was complete, individual components could be designed and built. This thesis will discuss detailed design, construction, and preliminary testing of critical components in the return portion of the wind tunnel: a 90-degree corner, the fan, and a diffuser. Corners are used in the wind tunnel to turn the flow so that the tunnel forms one continuous loop. To provide flow, a fan is utilized. Lastly, the diffusers are used to decrease the flow velocity in all regions except for where testing is taking place. Test results will be shown and future work discussed.

Thesis Supervisor: Dr. Kurt Aikens
Title: Aerodynamics Engineer

TABLE OF CONTENTS

| | |
|--|-----------|
| Chapter 1 Background on Wind Tunnels | 5 |
| 1.1. History of the Wind Tunnel | 5 |
| 1.2. Approaches to Fluid Mechanics | 8 |
| 1.3. Objective of this Project | 11 |
| Chapter 2 Theory | 13 |
| 2.1. Governing Equations | 13 |
| 2.2. Useful Approximations of the Governing Equations | 16 |
| 2.2.1. Bernoulli's Equation..... | 16 |
| 2.2.2. Quasi-One-Dimensional Flow..... | 17 |
| 2.3. Wind Tunnel Performance | 19 |
| 2.3.1. Loss Estimation Overview | 19 |
| 2.3.2. Corner Performance..... | 20 |
| 2.3.3. Diffuser Performance..... | 21 |
| Chapter 3 Wind Tunnel Apparatus | 25 |
| 3.1. Construction of the Wind Tunnel | 25 |
| 3.2. Building Corner 2 | 27 |
| 3.3. Diffuser Testing | 28 |
| Chapter 4 Experimental Results | 33 |
| 4.1. Wind Tunnel Diffuser Data Collection | 33 |
| Chapter 5 Conclusions and Future Work | 35 |
| 5.1. Conclusions | 35 |
| 5.2. Future Work | 35 |

TABLE OF FIGURES

| | |
|---|----|
| Figure 1. Diagram of Benjamin Robins Whirling Arm..... | 6 |
| Figure 2. Diagram of a plane being tested | 6 |
| Figure 3. Figure of the four identifying elements of a wind tunnel | 7 |
| Figure 4. Figure of Couette flow between two surfaces | 9 |
| Figure 5. An example of a mesh for CFD of fluid flow past an airfoil | 10 |
| Figure 6. Simulation grid of a segment of a centrifugal compressor | 10 |
| Figure 7. Depiction of a fluid control volume..... | 14 |
| Figure 8. Depiction of streamlines for steady flow through a diffuser | 17 |
| Figure 9. Figure of quasi-one-dimensional flow in a duct | 18 |
| Figure 10. Diagram of a typical wind tunnel corner..... | 21 |
| Figure 11. Image of air bubbles in water | 22 |
| Figure 12. Figure of a cone shaped diffuser | 23 |
| Figure 13. Graph showing regions of the design space for diffusers | 24 |
| Figure 14. Depiction of the Houghton College wind tunnel..... | 26 |
| Figure 15. Diagram of the cross section of the corner vanes | 26 |
| Figure 16. Image of an early attempt cutting the vanes | 27 |
| Figure 17. Diagram of the foam support form for the corner vanes. | 28 |
| Figure 18. Image of the completed corner vane assembly | 29 |
| Figure 19. Diagram of the vane cascade viewed from the side | 30 |
| Figure 20. Figure of a Pitot-static tube..... | 30 |
| Figure 21. Image of the Dwyer Mark II Manometer | 31 |
| Figure 22. Diagram of Diffuser 2 with 5 holes drilled above..... | 31 |
| Figure 23. Figure of the wind tunnel Diffuser 2 air velocity measurements..... | 33 |
| Figure 24. Image of the inside of the motor fan in the Houghton College wind tunnel ... | 34 |

Chapter 1

BACKGROUND ON WIND TUNNELS

1.1. History of the Wind Tunnel

Early researchers were inspired by the flight of birds. Their goal was to build a machine that would replicate the flight of a bird. This pursuit led to them to realize that to fly a machine, they would require more information on the interaction between the air and their device [1].

To improve their understanding, researchers needed access to a controlled airstream that allowed repeatable measurements to be taken. Natural winds are not sufficient in this regard, because they are rarely uniform or repeatable. One of the first apparatus designed for this purpose was the whirling arm, pictured in Figure 1. The whirling arm was first made by mathematician Benjamin Robins [1]. The object on the whirling arm spun by a falling weight acting on a pulley and spindle arrangement [1]. The whirling arm measured drag, which is a force acting opposite to the relative motion of any object, by spinning objects in a circular path. A depiction of the aerodynamic forces that act on an object in flight is shown in Figure 2. Once the object reaches constant speed and there is no angular acceleration, the torque produced by the drag counters the torque produced by the falling mass. With this information the drag force can be measured. To measure the lift force, the component of the force that is perpendicular to the oncoming flow direction, Robins would attach increasing amounts of weight to the object until it remained horizontal while spinning. The lift force then, equaled the total weight added. Robins tested various objects with different shapes and was able to determine that despite having the same frontal area exposed to the airstream, different shapes have different air resistance [1].

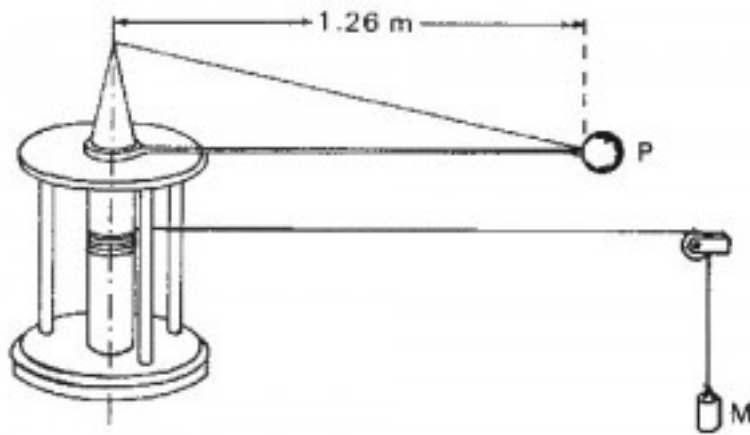


Figure 1. Diagram of Benjamin Robins Whirling Arm. This machine consisted of weight M which rotated the system and the test object P. Figure taken from Ref. [1].

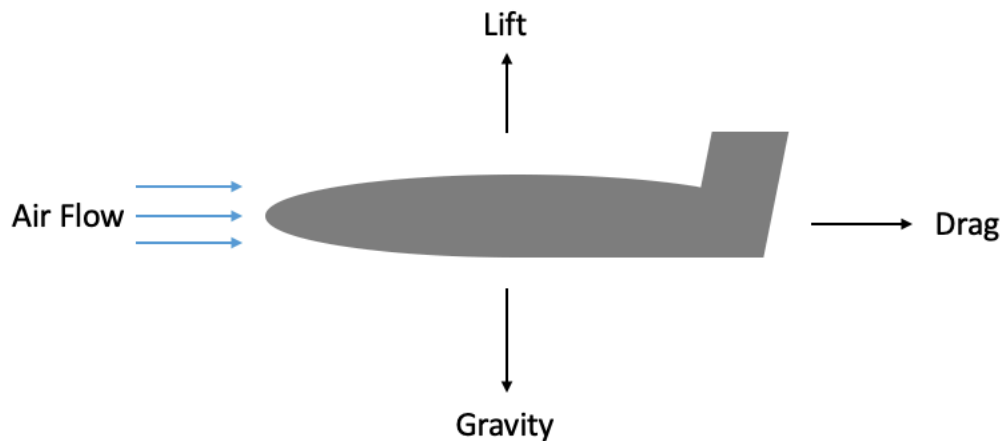


Figure 2. Diagram of a plane being tested, which shows air flow, lift, net force, and drag.

The whirling arm was a big step for aeronautics; it provided most of the aeronautic data of the 19th century. This information was crucial, but the whirling arm also had some flaws. When spinning the test models, the whirling arm would create a mass of air swirling around itself – an unsteady wake flow downstream from the moving model. As a result of this, the airflow that the model traveled through was not as uniform as was desired for accurate measurements. Furthermore, it made it difficult for experimenters to determine the relative velocity between the model and the air, because the air speed was not zero [1].

The need for more accurate measurements of the forces exerted on the test models led to the invention of the wind tunnel. Frank H. Wenham, a Council Member of the Aeronautical Society of Great Britain, is credited with designing the first wind tunnel [1]. The wind tunnel provides a flowfield that is more uniform than that produced by the whirling arm, and it is also more steady [1]. A wind tunnel consists of a fan that causes air to flow at high speeds through an enclosed passage. Despite various designs of the wind tunnel, it will always consist of four crucial elements: the drive system, test section, model, and test instrumentation; these elements can be seen in Figure 3. The drive system is usually a motor-driven fan that blows or pulls air through the wind tunnel. As shown in Figure 3, the fan pulls air through the test section where a model has been placed. While the air is flowing, the aerodynamic characteristics of the model can be measured using the test instrumentation in the test section [1].

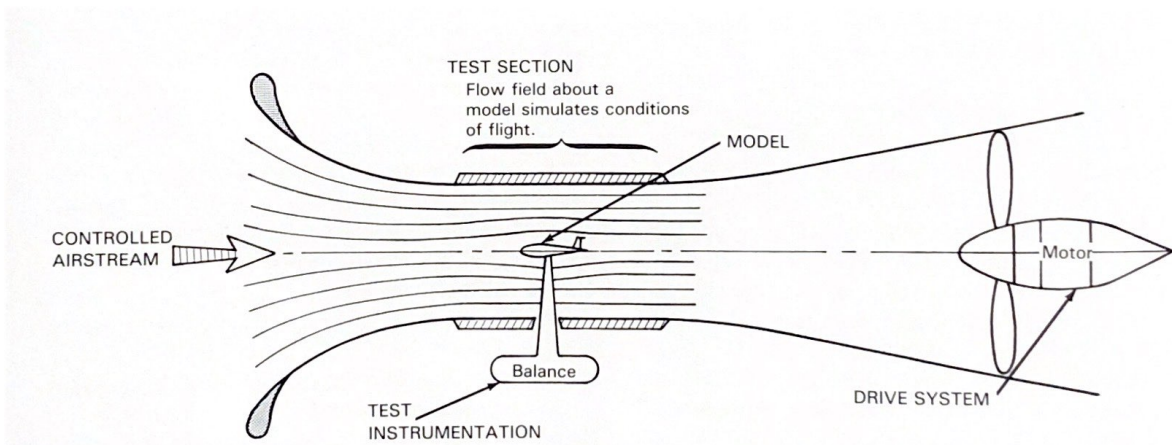


Figure 3. Figure of the four identifying elements of a wind tunnel. Every wind tunnel has them although the specific details vary greatly from one design to the next. Figure taken from Ref. [1].

The issue with the wind tunnel was that the test sections were too small to test full-sized objects. Of course, it would be desirable to test full-scale models, but it is often too expensive to do so [1]. Similar challenges remain with experimental fluid mechanics today. These are elaborated upon in the next section, and complementary approaches to aerodynamics are also discussed.

1.2. Approaches to Fluid Mechanics

In addition to the experimental approach to fluid mechanics which was introduced in the previous section, there are two others. The first is the theoretical approach, which is applying Newton's laws to the motion of a fluid. Progress in technology led to the development of the other approach, computational fluid dynamics (CFD), which approximates the solution to the equations that govern fluid dynamics. With the addition of CFD, there are now three methods that can be used to solve problems in aerodynamics [2]. Each of the methods will be discussed further in this section, including the advantages and disadvantages of each.

First, the theoretical approach involves analytically solving the laws of physics, applied to the motion of a fluid, for scenarios of interest. In the theoretical approach simplifying assumptions are made to make the problem tractable [2]. One of the advantages to the theoretical approach is that one can obtain reasonable answers in a minimum amount of time. The most important advantage, however, is that a theoretical solution is closed form. This is helpful because the variables that influence the solution are clear. It is also easy to examine how sensitive the solution is to these variables. If it were possible, the theoretical approach would be used for every scenario. The disadvantage of the theoretical approach is that one is limited to solving relatively simple problems where the governing equations become linear; analytical solutions simply do not exist for most practical engineering problems [2]. An example of a problem that has an analytical solution is the classic problem of Couette flow. Couette flow is the flow of a viscous fluid in the space between two surfaces, one of which is moving tangentially relative to the other [3]. An image of this is seen in Figure 4. The central assumption is that the two surfaces are infinitely large. Under this assumption, the governing equations become linear and an analytical solution to the resultant ordinary differential equation is possible. Of course, this exact scenario does not occur in nature. However, the solution is still applicable to scenarios where the surfaces are sufficiently large relative to the size of the gap between them.

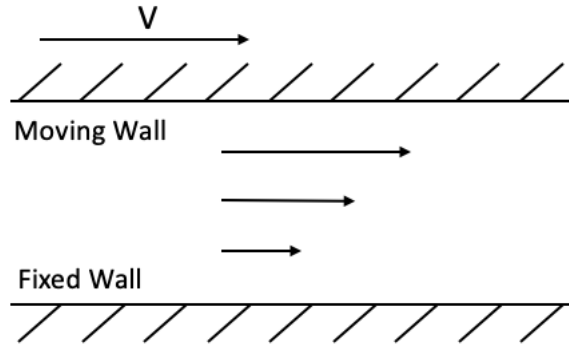


Figure 4. Figure of Couette flow between two surfaces. V represents the speed of the upper wall, and the arrows between the walls represent the fluid flow.

The second method, computational fluid dynamics (CFD) uses numerical methods to approximate the solution to problems in fluid mechanics. In CFD, only a limited number of physical assumptions are made and a high-speed digital computer is used to solve the governing equations of fluid dynamics [2]. There is no restriction to linearity and complicated phenomena can be solved [2,4]. Using CFD requires the division of the fluid region into cells. See Figure 5 for an example of a mesh used for a CFD analysis of an airfoil. The fluid properties, like density and velocity, are assumed to be uniform over each cell. The more cells used the better the result, but the more expensive the calculation will be. Not using enough cells can harm the accuracy of the simulation and can lead to truncation errors [5]. This illustrates one of the perpetual tradeoffs with CFD: accuracy versus expense. This also becomes important when it comes to physical modeling. For example, to directly solve for a turbulent flow with CFD, an impractically expensive direct numerical simulation (DNS) is required [2]. For nearly all applications, alternative turbulence models are utilized that introduce certain physical assumptions. As a result of these modeling assumptions, there are many phenomena for which CFD results can be unreliable. For example, a non-exhaustive list of flow phenomena that are difficult for CFD includes: multiphase flow, boiling, condensation, combustion, and turbulent flows with separation or transition [2]. Despite these downsides, CFD is used often because there are many problems for which using the theoretical approach is not possible. Figure 6 shows a segment of a centrifugal compressor. When looking at a complicated problem like centrifugal compressors, CFD is regularly used to analyze the complicated flowfield.

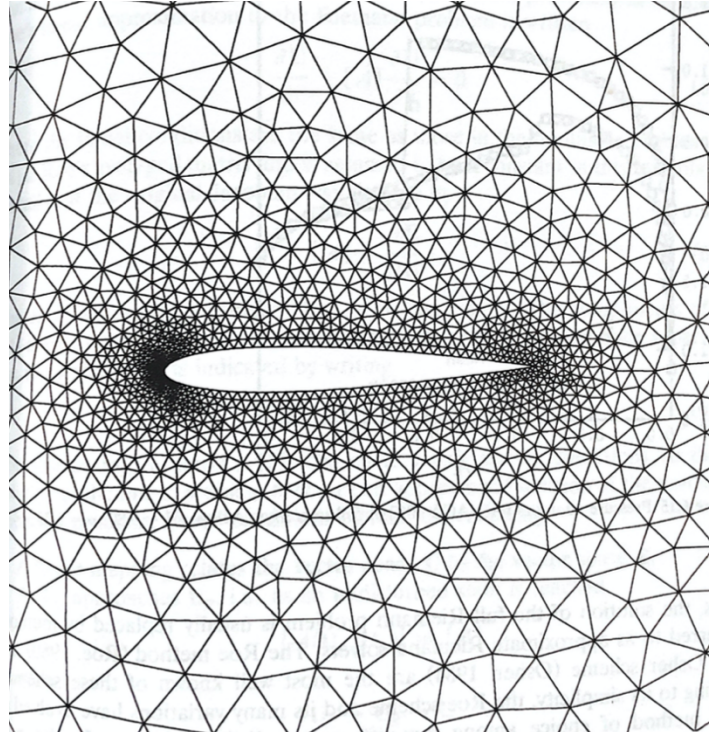


Figure 5. An example of a mesh for CFD of fluid flow past an airfoil. The fluid region has been divided into triangular-shaped cells. The fluid properties are assumed uniform over each cell, so more cells are required in regions where the gradient of fluid properties is large. Figure taken from Ref. [2].

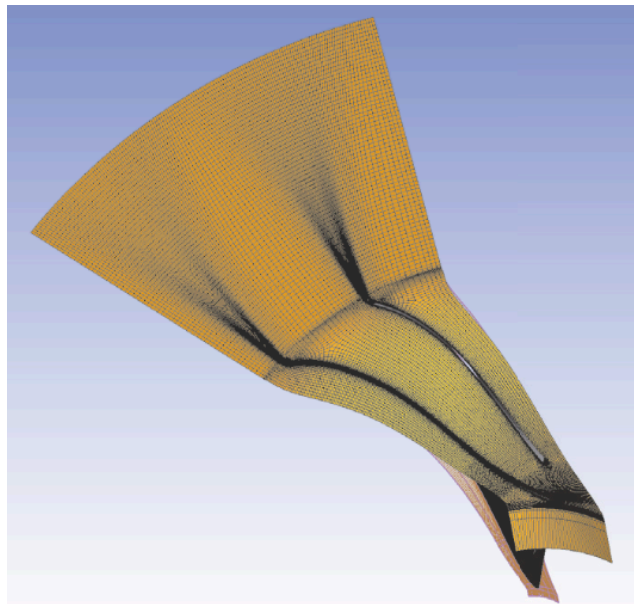


Figure 6. Simulation grid of a segment of a centrifugal compressor. Figure taken from Ref. [6].

Despite having theoretical and computational methods, the experimental approach is still used because it is capable of giving the most realistic results [2]. The experimental approach involves physically testing scaled models in a wind tunnel facility. Testing a small-scale model is acceptable because the measured lift, drag, and moment coefficients (i.e., the non-dimensional results) will be the same as for the full-scale vehicle in free flight as long as the Mach and Reynolds numbers for the test match those for the free flight case [4]. Despite the advantages of obtaining results from physical experiments, there are some disadvantages. First, when testing scale models, it is often difficult or impossible to perfectly match the Reynolds and Mach numbers to those of the full-scale scenario. This requires that resulting test data be interpreted carefully as effects that are sensitive to the Reynolds and/or Mach numbers may not be captured accurately. Second, it is not always possible to directly measure a desired quantity. For example, some fluid environments are too hazardous for survival of instrumentation (e.g., in the combustor of a jet engine). The last and most important limitation of the experimental approach is that experiments are extremely costly in terms of both money and time. Not only are expensive wind tunnels often required, but they cost money to run and tests can take months of meticulous planning and preparations. This is much longer than is typically required for theoretical and computational studies [2].

In practice, the theoretical, computational, and experimental approaches are all used to varying extents. This allows researchers to cross-check the results and improves confidence in final conclusions. This underscores the importance of having access to experimental resources.

1.3. Objective of this Project

The objective of this project is to continue previous efforts of designing and building a low speed wind tunnel. With a wind tunnel, Houghton College will have the capabilities of running its own fluid dynamics experiments. Examples of future tests might include studies of how tennis balls move through air, or how an aircraft handles turbulence. The wind tunnel will help students gain experience with experimental testing. As mentioned, this is important because fluid dynamics students need experience with the experimental method in addition to the theoretical and computational methods.

Through the work of previous students, general decisions about the Houghton College wind tunnel design were made. Jaramillo developed a MATLAB script that used empirically-based correlations to roughly size the wind tunnel given some basic design choices and constraints [7]. After a reasonable corner vane geometry was chosen, Eager used CFD to estimate the optimal number of turning vanes based on that geometry. His designs minimized the loss of energy through each corner [8]. Similarly, Martin analyzed three nozzles in CFD and determined which one was best for the wind tunnel. Martin determined this by considering the stagnation pressure drop across the nozzle and the flow uniformity produced in the test section [9]. Most recently, Durbin refined initial designs and began the construction of the wind tunnel [10].

This thesis follows the work done by these previous students. Building on the work of Eager [8], a corner vane cascade has been constructed and will be described here. Furthermore, preliminary measurements of the flow through one of the diffusers have been made to check that it is operating as expected. This project will also cover the general progress made on the wind tunnel and the steps still needed to complete it.

Chapter 2

THEORY

2.1. Governing Equations

When studying aerodynamics, there are basic equations that aerodynamicists need to know. Understanding these equations allows for better comprehension of the work described later in this thesis. The equations that govern the dynamics of fluids will be presented and explained in this section. The following discussion largely follows Anderson [4].

The continuity equation is one of the most fundamental equations of fluid dynamics. It applies the physical principle of the conservation of mass to a finite control volume fixed in space [4]. Figure 7 depicts an example of a control volume. The continuity equation in integral form is

$$\frac{\partial}{\partial t} \iiint_{\mathcal{V}} \rho d\mathcal{V} + \iint_S \rho \vec{V} \cdot d\vec{S} = 0 \quad (1)$$

where ρ is the fluid density, $d\mathcal{V}$ is an elemental volume inside the control volume, \vec{V} is the flow velocity, and $d\vec{S}$ is the vector elemental surface area. Within the first term is a volume integral of density; it is equal to the fluid mass within the control volume. The first term as a whole represents the time rate of change of mass within the control volume. The second term, then, describes how the amount of fluid mass inside the volume can change as fluid moves into or out of the boundary, S . If the fluid is moving into or out of the volume through S , the amount of mass within the volume changes.

The next governing equation represents conservation of momentum; it is developed from the use of Newton's second law applied to the motion of a fluid. The general form of Newton's second law is

$$\sum_k \vec{F}_k = \frac{d}{dt} (m\vec{V}). \quad (2)$$

Looking at the left hand side of Equation (2), the individual forces, \vec{F}_k , are of two fundamental types:

1. Body forces: gravity, electromagnetic forces, and other forces that act at a distance on the fluid inside \mathcal{V} .
2. Surface forces: pressure and viscous forces acting on the fluid along the control surface, S .

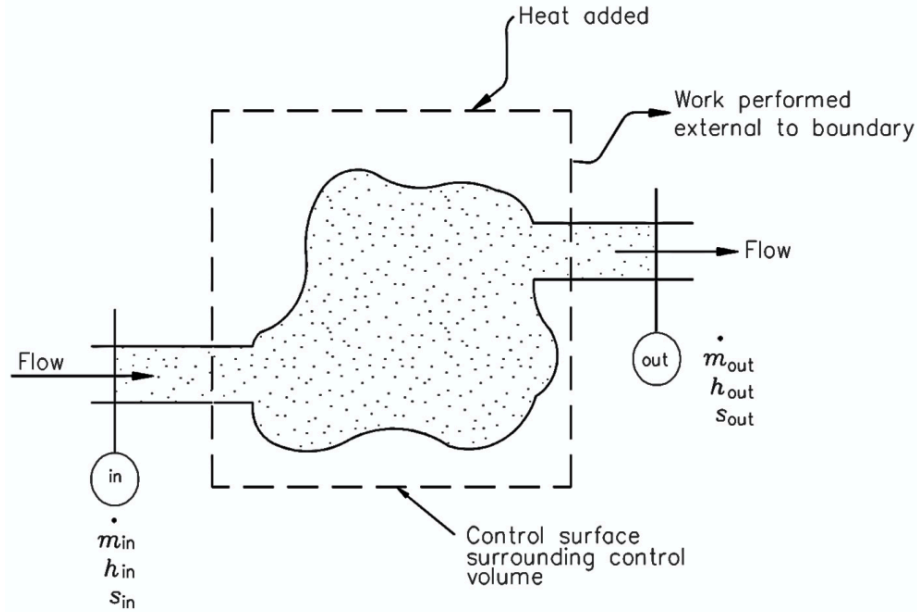


Figure 7. Depiction of a fluid control volume. Figure taken from Ref. [11].

The momentum equation in integral form is

$$\frac{\partial}{\partial t} \iiint_{\mathcal{V}} \rho \vec{v} dV + \iint_S (\rho \vec{v} \cdot d\vec{S}) \vec{v} = - \iint_S p d\vec{S} + \iiint_{\mathcal{V}} \rho \vec{f} dV + \vec{F}_{viscous} \quad (3)$$

where p is the pressure, \vec{f} is the net body force per unit mass exerted on the fluid inside \mathcal{V} , and $\vec{F}_{viscous}$ is the viscous force exerted on the fluid at the control surface. The first term in Equation (3) is the time rate of change of the momentum contained at any instant inside the control volume while the second term is the net flow of momentum in or out of the control volume through the surface. As such, the entire left side of the equation represents the time rate of change of momentum within the control volume – it represents the right hand side of Equation (2). The right side of Equation (3) represents the forces acting on the fluid. The first term on the right is the summation of the pressure force over the entire control surface, the

second term is the total body force on the fluid in the control volume, and the last term represents the contributions of viscous forces.

The last governing equation represents conservation of energy. The physical principle for this equation comes from the first law of thermodynamics. Energy can be neither created nor destroyed; it can only change in form [4]. The energy equation in integral form is

$$\begin{aligned} \frac{\partial}{\partial t} \iiint_V \rho \left(e + \frac{V^2}{2} \right) dV + \iint_S \rho \left(e + \frac{V^2}{2} \right) \vec{V} \cdot d\vec{S} \\ = \iiint_V \dot{q} \rho dV + \dot{Q}_{viscous} - \iint_S p \vec{V} \cdot d\vec{S} + \iiint_V \rho (\vec{f} \cdot \vec{V}) dV + \dot{W}_{viscous} \end{aligned} \quad (4)$$

where \dot{q} is the volumetric rate of heat addition per unit mass, $\dot{Q}_{viscous}$ is the rate of heat addition to the control volume due to viscous effects, $\dot{W}_{viscous}$ is the work performed on the fluid by viscous forces, and e is the internal energy per unit mass. Looking at the left-hand side of Equation (4), the first term is the time rate of change of total energy inside the volume (i.e., internal energy plus kinetic energy) due to transient variations of flow-field variables. The second term is the net rate of flow of total energy across the control surface. The first term on the right-hand side is the rate of volumetric heating, and when added with $\dot{Q}_{viscous}$ it is the total rate of heat addition. The third term is the rate of work done on the fluid inside the volume due to pressure force on the surface. Similarly, the fourth and fifth terms represent the work done by body forces acting on the fluid throughout the control volume and viscous forces along the control surface, respectively.

Stated above are the equations of continuity, momentum, and energy. Together these equations have seven dependent variables: ρ , p , e , temperature, and \vec{V} , which has three components. The previous equations only represent five equations; therefore, two more equations are needed to close the set of equations. In many cases, it can be assumed that the gas is a perfect gas with constant specific heats. Under these assumptions

$$e = c_v T, \quad (5)$$

where c_v is the specific heat at constant volume and T is the temperature, and

$$p = \rho RT, \quad (6)$$

where R is the specific gas constant. With the addition of Equations (5) and (6) to Equations (1), (3), and (4), the fundamental equations of fluid flow form a closed set of equations.

2.2. Useful Approximations of the Governing Equations

2.2.1. Bernoulli's Equation

Bernoulli's equation is one of the most famous equations in fluid dynamics. It marked the first time where a relationship between pressure and velocity in an incompressible fluid with negligible viscosity was first understood [4]. Bernoulli's equation is derived from the conservation of energy and was first presented by Euler [12] (see Ref. [13] for an English translation) as

$$p + \frac{1}{2}\rho V^2 = \text{constant}, \quad (7)$$

where p is pressure (also known as the static pressure), ρ is density, V is velocity magnitude, and the constant is referred to as the total pressure or stagnation pressure. The pressure in Equation (7) represents a new form of potential energy that fluids have, the second term represents kinetic energy, and the total pressure represents the total energy which is constant. Bernoulli's equation can also be written as

$$p_1 + \frac{1}{2}\rho V_1^2 = p_2 + \frac{1}{2}\rho V_2^2. \quad (8)$$

Equation (8) relates p_1 and V_1 at point 1 on a streamline to p_2 and V_2 at another location, point 2, on the same streamline. A series of streamlines is shown in Figure 8. For reference, streamlines are curves whose tangent at any point is in the direction of the velocity vector at that point [4]. It should be noted that if the flow is assumed to be irrotational (i.e., the curl of the velocity is zero), the equation applies to any two points in the flowfield.

Bernoulli's equation is useful for understanding the operation of wind tunnels. In some situations, the viscous losses can be assumed to be negligible. In other cases, where the losses are not small, the losses will produce a drop in the total pressure of the fluid.

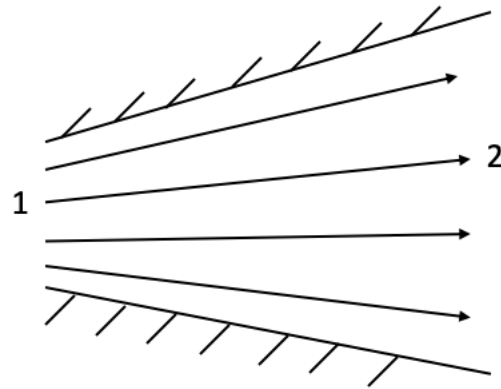


Figure 8. Depiction of streamlines for steady flow through a diffuser.

2.2.2. Quasi-One-Dimensional Flow

Similar to Bernoulli's equation in the previous section, a more useful form of the continuity equation can also be obtained by making additional assumptions about the flowfield in a wind tunnel. Quasi-one-dimensional flow considers the flow-field variables to be a function of only one spatial dimension. Strictly speaking, the flow in wind tunnels is fully three dimensional. However, if it is assumed that the flowfield variation in the transverse directions is negligible (i.e., the flow is uniform at each streamwise location), the flow essentially becomes one dimensional [4]. Under this assumption, a closed-form solution to the continuity equation can be obtained.

Figure 9 shows a situation where the quasi-one-dimensional assumption can be applicable. The area of the passage, A , is a function of x . Therefore, the fluid properties (density, pressure, etc.) are also functions of x . Equation (1) for steady flow (i.e., there is no time-dependence, so the first term is zero) becomes

$$\iint_S \rho \vec{V} \cdot d\vec{S} = 0. \quad (9)$$

Equation (9) can be applied to the duct in Figure 9. In this figure the control volume is bounded by cross-sectional areas A_1 on the left, A_2 on the right, and the upper and lower walls of the duct [4]. Therefore, Equation (9) can be written as

$$\iint_{A_1} \rho \vec{V} \cdot d\vec{S} + \iint_{A_2} \rho \vec{V} \cdot d\vec{S} + \iint_{A_{walls}} \rho \vec{V} \cdot d\vec{S} = 0. \quad (10)$$

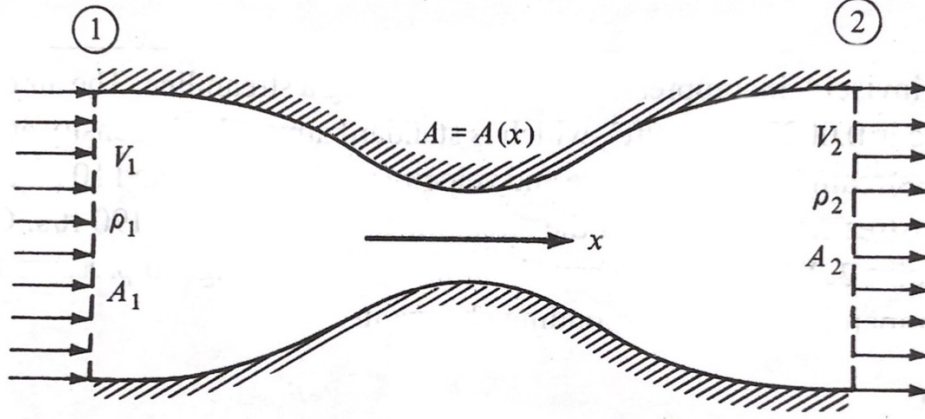


Figure 9. Figure of quasi-one-dimensional flow in a duct. As the cross-sectional area, A , changes with x , the flow variables do also. Figure taken from Ref. [4].

The velocity at the wall cannot have a component into or out of the wall by definition. Therefore, the fluid velocity and $d\vec{S}$ are perpendicular at each point along the wall, and $\vec{V} \cdot d\vec{S} = 0$. This means that the last integral term in Equation (10) is zero. The remaining terms can be simplified if an important assumption is made: the flow properties are uniform at each x value (i.e., at each streamwise location). Noting that since $d\vec{S}$ and \vec{V} are in opposite directions at station 1 of Figure 9, the first integral term in Equation (10) becomes

$$\iint_{A_1} \rho \vec{V} \cdot d\vec{S} = -\rho_1 A_1 V_1. \quad (11)$$

The same uniform flow assumption can be made over area A_2 in Equation (10). Since $d\vec{S}$ and \vec{V} are in the same direction in station 2, the equation can be written as

$$\iint_{A_2} \rho \vec{V} \cdot d\vec{S} = \rho_2 A_2 V_2. \quad (12)$$

Note that the assumption that the flow variables are uniform over the cross-sectional area is required for Equation (11) and Equation (12). Substituting both into Equation (10) produces

$$\rho_1 A_1 V_1 = \rho_2 A_2 V_2. \quad (13)$$

Equation (13) is the quasi-one-dimensional continuity equation. In some cases, it is reasonable to further assume that the flow is incompressible – that ρ is constant. This is generally a good assumption for low speed (i.e., low Mach number) wind tunnels. Therefore, Equation (13) can be simplified to

$$A_1 V_1 = A_2 V_2. \quad (14)$$

Equation (14) is the quasi-one-dimensional continuity equation for incompressible flow.

It should be clarified that the key assumption here – assuming that the flow-field variables are only functions of x – can break down [4]. If, for example, there is a sudden expansion or contraction, the flow variables will not be uniform over each x =constant plane. The most extreme example of this is if the flow separates. Under this condition, the flow detaches from the wall leaving a high velocity core and an approximately zero velocity wake near the wall.

2.3. Wind Tunnel Performance

As previously discussed, the wind tunnel is composed of multiple sections. Each section contributes to the overall function of the wind tunnel. In Section 2.2.1, Bernoulli's equation was introduced. Under ideal conditions (i.e., no fluid viscosity), the total pressure of a fluid is constant. In practice, the flow in a wind tunnel experiences a loss in energy, and therefore total pressure, when it flows through a given section. The purpose of this section is to introduce general loss estimations for common wind tunnel components. Specifically, losses in diffusers and corners will be expanded upon because they are relevant to the work completed as part of this project. For a more detailed summary of losses in wind tunnel components, see Barlow, et al. [14].

2.3.1. Loss Estimation Overview

The loss in a section is defined as the mean loss of total pressure sustained by the flow as it passes through that section [14]. The loss coefficient is given in dimensionless form by the ratio of the pressure loss in the section to the dynamic pressure at the entrance to the section,

$$K = \frac{\Delta p_0}{\frac{1}{2} \rho V_1^2}. \quad (15)$$

In Equation (15), Δp_0 is the drop in total pressure, V_1 is the velocity magnitude at the beginning of the component, and ρ is the density of the fluid. This is a convenient form for the loss coefficient because the total pressure loss and the dynamic pressure are easily measurable. Furthermore, for many wind tunnel components, the loss coefficient is independent of or only weakly dependent on the fluid velocity. This makes the loss coefficient easier to develop a model for than the total pressure loss directly. A side effect of the loss coefficient being approximately independent of the fluid velocity is that the total pressure loss scales as the velocity squared. Therefore, it is very beneficial to minimize flow velocities in all portions of the wind tunnel where a high velocity is not needed. This idea will be expanded upon while talking about diffusers.

2.3.2. Corner Performance

The corners in wind tunnels can produce large losses compared to other components. A diagram of what corners often look like is seen in Figure 10. To avoid significant loss, turning vanes need to be implemented into the wind tunnel. Also, as mentioned in the previous section, corners should be located in a large-area section where the flow speed is low. Losses can be further reduced in corners in two ways: (1) by selecting an efficient vane cross-sectional shape and adjusting it for proper alignment with the flow, and (2) by choosing the best chord-to-gap ratio [14].

The specific loss coefficient empirical model for corners, as developed by Wattendorf [15], is

$$K_c = 0.10 + \frac{4.55}{(\log_{10} Re_c)^{2.58}} \quad (16)$$

where Re_c is the local Reynolds number based on the corner vane chord length, c ,

$$Re_c = \frac{\rho V_1 c}{\mu_1}, \quad (17)$$

where μ_1 is the viscosity. The Reynolds number has a powerful influence over the properties of a boundary layer and viscous flows in general [4]. Equation (16) decreases as the Reynolds number increases. While Equation (16) does not capture the influence of the shape of the corner vanes or the spacing between them, it gives a reasonable preliminary estimate for the loss coefficient value.

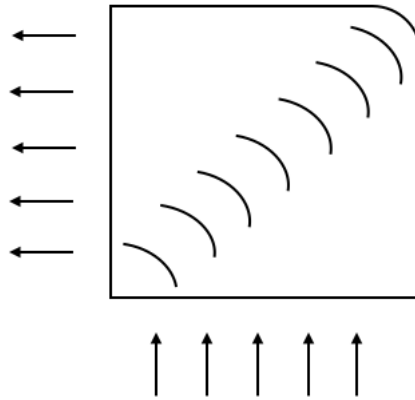


Figure 10. Diagram of a typical wind tunnel corner showing vanes which help turn the flow 90 degrees. The arrows represent the flow. Corner vanes, when properly designed and implemented, improve flow uniformity and minimize total pressure losses.

2.3.3. Diffuser Performance

The diffuser is a wind tunnel component where the flow goes from a small cross-sectional area to a larger one as seen in Figure 8. Therefore, according to the quasi-one-dimensional continuity equation, Equation (13), the fluid velocity decreases through the diffuser and is therefore lower for all downstream components. This helps reduce losses in components downstream of the diffuser.

However, diffusers must be designed with care. Given that the velocity decreases through the diffuser, Bernoulli's equation (Equation (7)) shows that the pressure correspondingly increases. This is referred to as an adverse pressure gradient, and it can produce flow separation. Flow separation occurs when the fluid detaches from the wall of the diffuser. An image showing fluid separation is seen below in Figure 11. Separation like this can cause vibrations, oscillations in flow velocity throughout the wind tunnel, oscillatory fan loading, and higher losses in downstream components [16].

To avoid flow separation, the equivalent cone angle and area ratio of the diffuser must be properly selected. Using the equivalent cone angle, θ_e , the diameters of the ends of the cone diffuser match the hydraulic diameter of the rectangular diffuser. A figure of a cone shaped diffuser is seen in Figure 12. Mathematically,

$$\theta_e = \arctan\left(\frac{R_d - R_u}{L}\right) = \arctan\left(\frac{1}{2} \frac{\sqrt{A_r} - 1}{L/D_u}\right), \quad (18)$$

where R_d and R_u are the downstream and upstream radii of the diffuser, L is the length of the diffuser, A_r is the diffuser area ratio A_d/A_u , and D_u is the hydraulic diameter at the upstream end. For diffusers that are not conical, the radii in Equation (18) should be replaced with half the hydraulic diameter of the upstream and downstream areas. The hydraulic diameter for a rectangular cross-section is defined by Blevins [18] as

$$D = \frac{2lw}{l + w}, \quad (19)$$

where l and w are side lengths.

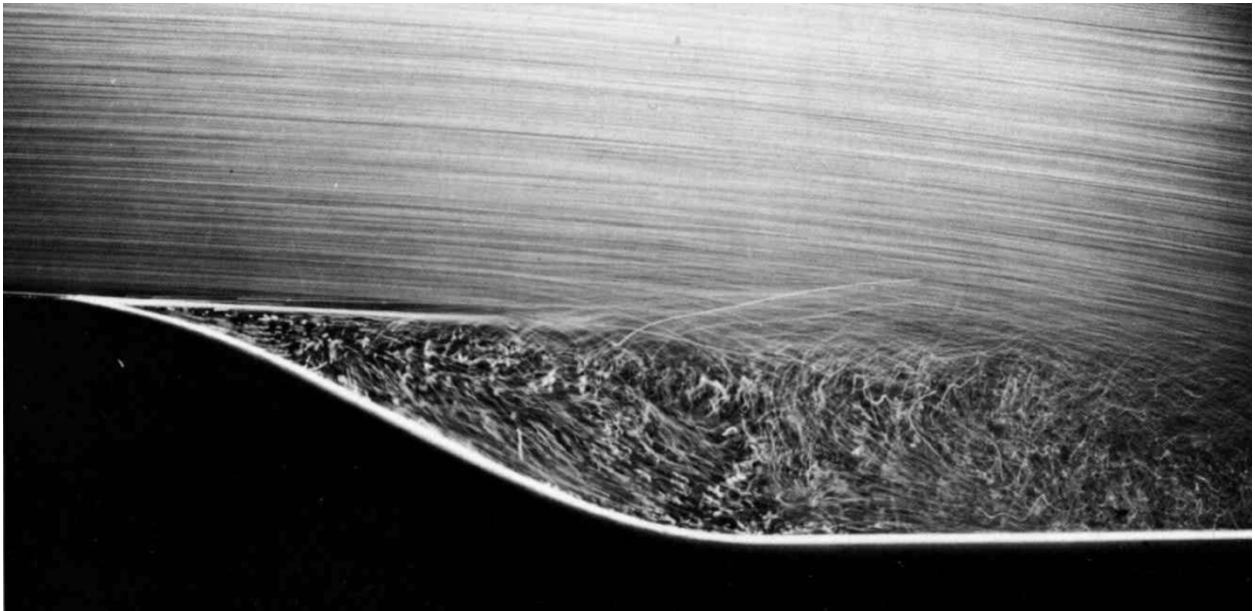


Figure 11. Image of air bubbles in water shows the separation of a laminar boundary layer. Because it is free bubbles, the boundary layer appears as a dark line at the left. The flow area is increasing, as the flow travels from left to right, similar to what occurs in a diffuser. In this case, the area expansion occurs so rapidly that the boundary layer separates tangentially near the start of the convex surface. The boundary layer remains laminar for the distance to which the dark lines persist, and then it becomes unstable and turbulent. Notice that the bubbles in the separation region follow chaotic patterns unlike those in the laminar portions of the flowfield. Figure taken from Ref. [17].

The main constraint on the angle is that it be small enough so that the turbulent boundary layer does not separate [14]. Barlow et al. [14] recommend that the typical equivalent cone

angle be in the range of 2-3.5°, and that the area ratio be between 2-3. Blevins [18] defines guidelines based on the area ratio and the length of the diffuser. Figure 13 shows his area ratio vs. non-dimensional length guidelines for three different kinds of diffusers: annular, conical, and two-dimensional. The non-dimensional length is defined as

$$L' = \frac{L}{R_u}. \quad (20)$$

In Figure 13, the area to the bottom right of a given curve shows the portion of the design space where the diffuser should avoid "stall" – boundary layer separation. The upper right hand, alternatively, shows the combinations of area ratio and non-dimensional length where appreciable separation is likely. This is qualitatively similar to the guidelines from Barlow et al. Large area ratio diffusers that are short (i.e., have a large equivalent cone angle) are the most likely to have separation present. The design of the diffusers for the Houghton College wind tunnel are closest to a conical diffuser and will be compared to these guidelines in Chapter 3.

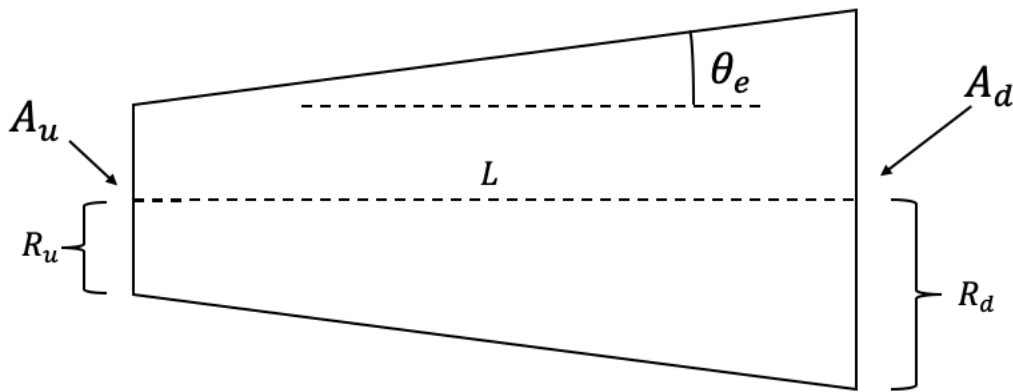


Figure 12. Figure of a cone shaped diffuser. A_u is the upstream area, and A_d is the downstream area. R_u and R_d are the radii of the upstream and downstream areas, respectively. L is the length of the diffuser.

For the purpose of modeling losses in diffusers, two kinds of losses occur: wall friction and expansion losses. The loss coefficient is often defined as the sum of a friction loss coefficient and an expansion loss coefficient indicated by Barlow et al. [14] as

$$K_d = K_f + K_{ex} \quad (21)$$

where

$$K_f = \left(1 - \frac{1}{A_r^2}\right) \frac{f}{8 \sin \theta_e} \quad (22)$$

and

$$K_{ex} = K_e(\theta_e) \left(\frac{A_r - 1}{A_r}\right)^2. \quad (23)$$

In Equation (21), K_f represents the unavoidable losses due to the fact that there is friction between the walls and the fluid. f is defined as the friction coefficient. K_{ex} , the expansion loss coefficient, is represented as a product of two factors. One factor, $K_e(\theta_e)$, is a function of the equivalent conical angle [14]. The second factor is a function of diffuser area ratio, A_r . For both terms, losses increase as the area ratio increases. This loss modelling all assumes that there is no fluid separation. If any separation is present, the total pressure loss increases dramatically. For more information on this, see Barlow et al. [14].

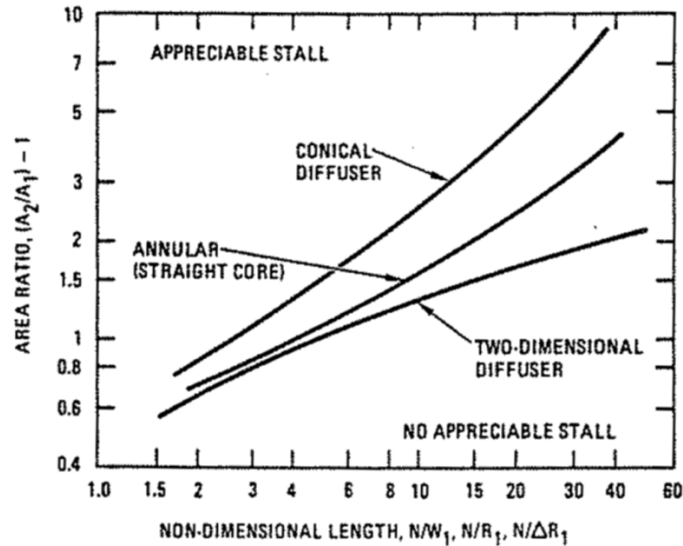


Figure 13. Graph showing regions of the design space for diffusers where separation is likely and unlikely to occur. To avoid stall, the allowable diffuser area ratio is a function of non-dimensional length. Graph taken from Ref. [18].

Chapter 3

WIND TUNNEL APPARATUS

3.1. Construction of the Wind Tunnel

Deciding whether to make an open return wind tunnel or a closed return wind tunnel was one of the first questions faced by researchers at Houghton College. Due to the small size of the laboratory space, an open return wind tunnel was impractical. Open return wind tunnels effectively use the room as the return portion for the wind tunnel, so using a small room for this produces larger losses [7]. The closed return wind tunnel, when properly designed and built, can also offer better results than its open return counterpart. While more expensive to build, they can be more efficient and produce more uniform test section flow. Ultimately, a closed-return design was chosen, and the current design is depicted in Figure 14.

While designing the Houghton College wind tunnel, the losses for each component were modeled using the loss coefficients described in Section 2.3 for corners and diffusers. Loss coefficients for the other components were obtained from Barlow et al. [14]. A Matlab script was developed to estimate the flow losses and evaluate many competing designs [7]. Once a specific design was chosen, an appropriately sized wind tunnel fan was acquired.

A few of the components in Figure 14 are especially important to the work completed here: the corners, the transitions, and the second diffuser. Each corner will have a series of corner vanes as seen in Figure 10. Work from previous student Daniel Eager [8] helped determine the number of vanes that produced the minimal total pressure drop. This scenario also approximately corresponds to the most uniform flow downstream of the corners. Due to its advantageous aerodynamic properties, an airfoil corner vane cross section was chosen. The specific vanes used here can be seen in Figure 15. Using CFD simulations, Eager found that 13 vanes were needed for Corners 1 and 2, and 19 vanes were needed for Corners 3 and 4. With regards to the transitions on either side of the fan, they are designed to maintain approximately constant cross-sectional area, but transition from a circular cross section to a

square one. The rest of this chapter will introduce the detailed design of a corner vane assembly and preliminary testing of the two transitions, the fan, and Diffuser 2.

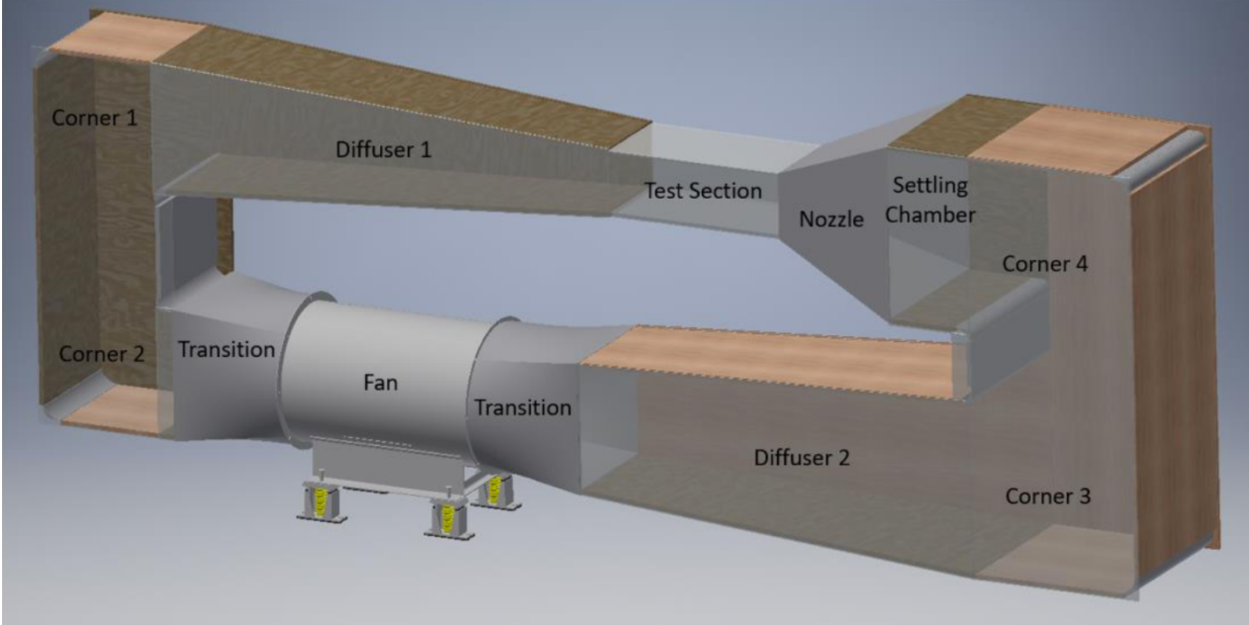


Figure 14. Depiction of the Houghton College wind tunnel with various components labeled. Figure taken from Ref. [10].

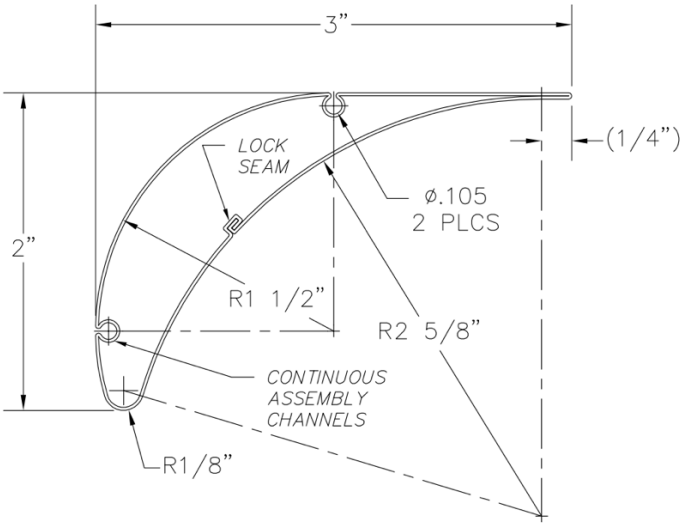


Figure 15. Diagram of the cross section of the corner vanes used in the Houghton College wind tunnel. This geometry is the High Efficiency Profile (H-E-P) Turning Vane designed and sold by Aero-Dyne.

3.2. *Building Corner 2*

After the optimal number of corner vanes was estimated by Eager [8], construction could begin. Each vane needed to be cut to 19.5 in. lengths for Corners 1 and 2 (see Figure 14). The decision to start with Corners 1 and 2 was made because those corners are smaller and require fewer and shorter corner vanes. This allowed for less waste if something went wrong. Using a Jet 414471 HBS-1321W, 13" x 21" Semi-Auto Horizontal Bandsaw, the initial attempts to cut the vanes led to substantial deformations of the vane geometry. Figure 16 shows an example of the deformation.



Figure 16. Image of an early attempt cutting the vanes.

To reduce the amount of deformation, the speed was optimized to decrease the rate at which the saw cut through the material. This, however, was not successful and a different approach was necessary. A dense foam was purchased from the company Smooth-On: their Smooth-On's FOAM-iT!™ 10 product. The mixture of the product will expand to approximately six times its original volume. Duct tape was placed over one end of the vane to seal it, and the mixture was added from the other end. The necessary amount of foam was estimated such that the vane would be filled on the inside once the foam had fully expanded and cured. Once filled, the vane was much more rigid and did not deform easily when cut with the bandsaw. As an added benefit of this extra rigidity, this will decrease the likelihood of the vanes deforming or vibrating during operation of the wind tunnel. In addition to filling the vane, a

support form was made from the foam to help with securing the vane on the bandsaw. A diagram of this is shown in Figure 17.

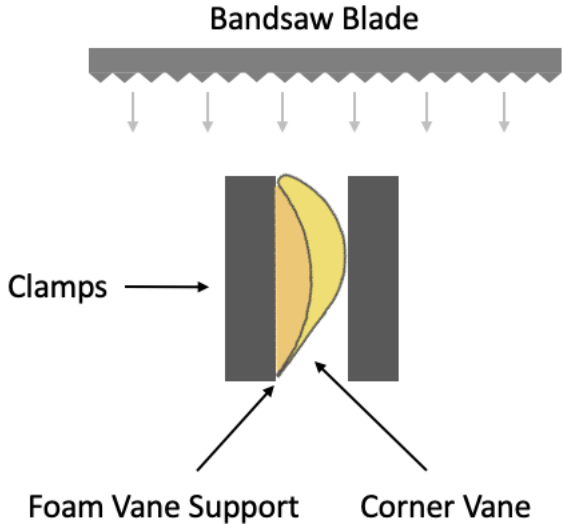


Figure 17. Diagram of the foam support form for the corner vanes.

After cutting the vanes to their appropriate length, they were assembled and made into a vane cascade with plexiglass on either end as seen in Figure 18. Holes were cut into the plexiglass to align with the desired positions of the holes in the vanes. The vanes were then fixed to the plexiglass using the Hillman Group 532590 4D, 1.5 in. nails. The diameter of the nails were 0.109 in., while the corner vane holes were 0.105 in. (see Figure 15). Building the vanes into an assembly like this allows for them to be installed and/or removed from the rest of the wind tunnel as a group. The vanes could then easily be replaced if they were damaged somehow, and there would be no need to rebuild the entire corner. Once the vane cascade is installed, the corners will look like Figure 10 from the top and Figure 19 from the side.

3.3. Diffuser Testing

After building Diffuser 2 as seen in Figure 14, a pitot-static tube was used to measure velocities and check for flow separation in the diffuser. Flow separation is noticed when there are areas in the diffuser where the flow velocity is close to zero. A Pitot-static tube is an instrument used to measure the difference between the total pressure and the static pressure. With the result from the Pitot-static tube and the fluid density of the air in the

laboratory, the flow velocity is calculated using Equation (8). Bernoulli's equation is valid here as the flow away from the walls should remain approximately irrotational (i.e., the curl of the velocity is zero in the interior of the flow). A Pitot static tube is depicted in Figure 20. Figure 21 shows the Dwyer Mark II Manometer which was used to measure the difference between the total and static pressure.



Figure 18. Image of the completed corner vane assembly. Notice the tan-colored foam that fills each corner vane.

To understand how a pitot-static tube operates refer to Figure 20. Hole A is exposed to the total pressure, which is defined as the fluid pressure when the fluid is brought to rest. The fluid at A cannot move into the probe because it is sealed, and the flow splits about that point. The holes at location B are exposed to the fluid moving at speed V , where the fluid pressure is the static pressure. Hole A is attached to channel 1 and the holes at B are attached to channel 2. This way, the higher pressure at A causes the fluid in the manometer to be pushed from high to low.

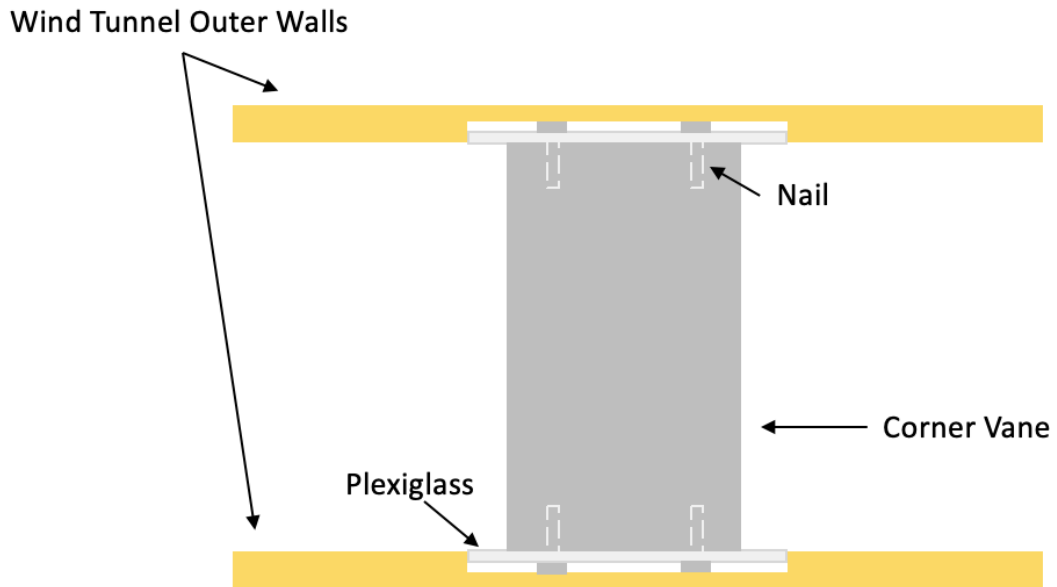


Figure 19. Diagram of the vane cascade viewed from the side once it has been installed into a corner.

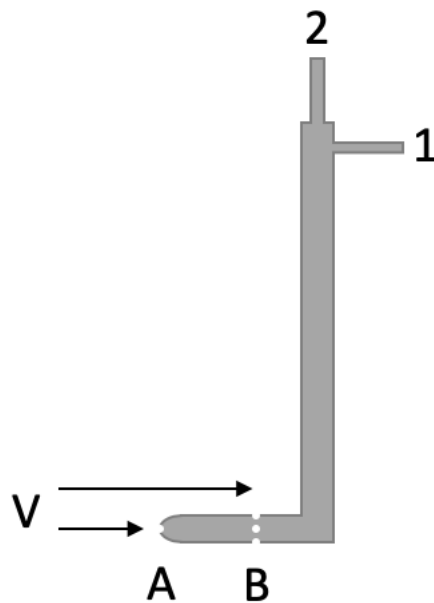


Figure 20. Figure of a Pitot-static tube. A is the point that is exposed to the total pressure. B is where the static pressure is measured. The arrows represent air flow. Channels 1 and 2 are connected to the manometer.

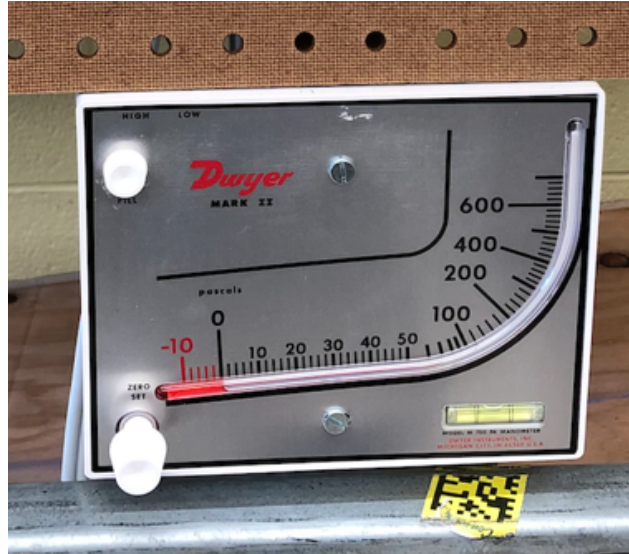


Figure 21. Image of the Dwyer Mark II Manometer.

The difference in pressures was measured at different distances from the inlet and different depths at each distance. Five holes were drilled into the top of Diffuser 2 at the locations depicted in Figure 22. The holes were separated by approximately 35 cm. The pitot-static tube was inserted in increments of 2 cm in each hole. The first distance was at 6 cm downstream of the inlet to ensure that the nose of the pitot-static-tube was completely within the diffuser. While not in use, the holes were plugged using rubber stoppers.

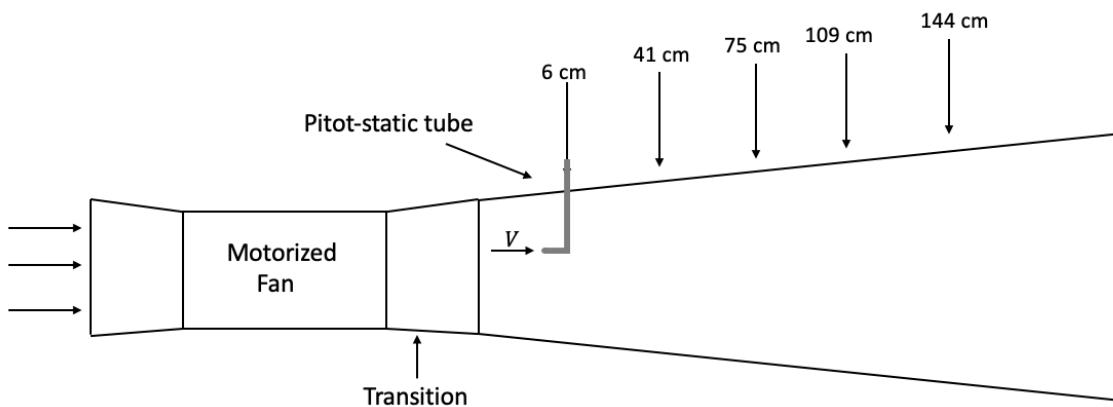


Figure 22. Diagram of Diffuser 2 with 5 holes drilled above. The numbers represent the distance of each hole from the start of the diffuser. V is the local fluid velocity, and the arrows represent air flow.

After this testing, the data was analyzed to calculate the velocity at each location and check for signs of separation. It is expected and hoped that there will be no separation because of

the guidelines followed in Section 2.3.3. Diffuser 2 has an equivalent cone angle of 3.12° , area ratio of 1.91, and the non-dimensional length is 6.98. Given the guidelines in Figure 13 for a conical diffuser (the closest approximation to the present diffuser design) and this non-dimensional length, the maximum area ratio Diffuser 2 can have is approximately three. The present value of 1.91, therefore, provides ample safety margin. The guidelines from Barlow et al. are also met because the equivalent cone angle is less than 3.5° and the area ratio is less than three. The velocity measurement results are presented and discussed in Chapter 4.

Chapter 4

EXPERIMENTAL RESULTS

4.1. Wind Tunnel Diffuser Data Collection

As seen in Figure 22, five holes were drilled in the top of Diffuser 2. These holes are 6 cm, 41 cm, 75 cm, 109 cm, and 144 cm from the upstream end of the diffuser, respectively. At each hole the pressure difference was measured in depth increments of 2 cm. The fan used was manufactured by New York Blower. It was a Vaneaxial, 21" Diameter, Arrangement 4M, 33-degree blade pitch fan. The motor for the fan was 7.5 HP with a max speed of 3600 rpm. A variable frequency drive (VFD) was used to control the fan. The VFD was manufactured by Safronics, and was their C10 2007-1, AC Vector Drive model. The speed of the fan was set to 30 Hz, yielding a fan rotational speed of approximately 1750 rpm. Figure 23 shows the results of this experiment. The air velocity is plotted on the x-axis and distance from the center of the wind tunnel was calculated and plotted on the y-axis.

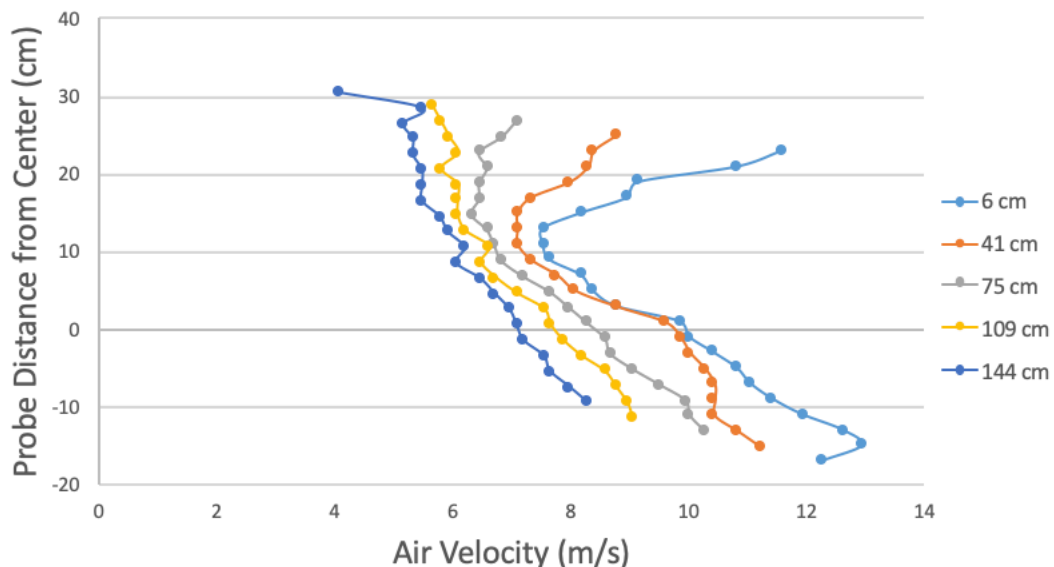


Figure 23. Figure of the wind tunnel Diffuser 2 air velocity measurements. Results are plotted at different distances downstream from the diffuser entrance.

From these results, it is observed that the air speed in the diffuser gets slower the further the pitot-static tube is from the fan. The purpose of the diffuser is to slow down the air flow by expanding the cross sectional area (see Section 2.2.2), so this result is expected. With that said there are a couple of interesting features in the results. First, the locations closest to the fan have a region of reduced flow velocity near the middle of the diffuser. This happened because the motor for the fan blocks the flow of air through the center of the diffuser. This is shown in Figure 24. The further the pitot-static tube was from the fan the less obvious this feature is. The second strange feature is that the flow is not symmetric from top to bottom as might be expected. There are a couple of reasons why this might be. One issue that can be seen in Figure 24 is that there are additional components in the flow path that could contribute to blockage: the plate on which the fan is mounted, a box on the right side of the image, and a power cable that connects on the right. Another issue is that the flow, especially near the fan, has a considerable amount of swirl. This decreases the accuracy of the measured velocity. To accurately measure the velocity, the pitot-static-tube would need to be pointed antiparallel to the fluid velocity. No attempt was made to do this in the experiment. Nevertheless, the results in Figure 23 are still meaningful. Specifically, they show that there are no areas where the flow approaches zero velocity. This suggests that there are no large regions of separation in the diffuser at this operating condition.



Figure 24. Image of the inside of the motor fan in the Houghton College wind tunnel. This image is taken from a perspective looking upstream through the diffuser towards the fan.

Chapter 5

CONCLUSIONS AND FUTURE WORK

5.1. Conclusions

In this work, the history of the wind tunnel was reviewed and the experimental approach was compared and contrasted with the other approaches to problems in fluid mechanics. Because experiments continue to be important, a wind tunnel is being developed at Houghton College. Past work on the wind tunnel was reviewed and current work on the wind tunnel was discussed. The objective of this project was to build a corner vane assembly to implement at each corner of the wind tunnel. This was done by filling each vane segment with rigid foam, and cutting them to the appropriate length. The vanes were then built into a removable cascade that will be installed into the wind tunnel corners.

This project also included testing Diffuser 2 and checking for regions of separation. The results showed that the diffuser flow velocity qualitatively follows the results of the quasi-one-dimensional continuity equation: as the area increased, the velocity decreased. There were also no large regions of flow separation seen in the results.

5.2. Future Work

Future work includes completing the vane assemblies for each of the corners, and finishing the construction of the rest of the wind tunnel. There is also considerable work required on choosing instrumentation to implement in the test section. Currently in consideration is mounting the tested object to a balance. A wind tunnel balance measures the aerodynamic forces and moments that a model experiences in the test section. A challenge that comes with balances is that the various force and moment components can vary widely in value at any given air speed [14]. If one is not careful, a given load component can exceed the structural limitations of the balance. The solution to this problem is to have several balances that are designed and built for different load ranges so that an appropriate one can be selected depending on the situation [14].

Once the wind tunnel is complete, it can be used for a variety of experiments. These experiments can aid existing classes at Houghton College, as well as make way for future aerodynamics and fluid mechanics courses. The wind tunnel can also make more opportunities for current students to perform research through the Houghton College Summer Research Institute.

References

-
- [1] D. D. Baals and W. R. Corliss, *Wind Tunnels of NASA*, 1st ed. (Scientific and Technical Information Branch, National Aeronautics and Space Administration, Washington, D.C., 1981).
- [2] D. Anderson, R. H. Pletcher and J. C. Tannehill, *Computational Fluid Mechanics and Heat Transfer*, 2nd ed. (Taylor & Francis, 1997).
- [3] F. Durst, *Fluid Mechanics: An Introduction to the Theory of Fluid Flow* (Springer-Verlag Berlin Heidelberg, 2008).
- [4] J. D. Anderson, *Fundamentals of Aerodynamics*, 4th ed. (McGraw-Hill, Boston, 2001).
- [5] J. Slotnick, A. Khodadoust, J. Alonso, D. Darmofal, W. Gropp, E. Lurie, D. Marvriplis, NASA CR 218178 (2014).
- [6] B. Dewar, J. Tiainan, A. Jaatinen-Värri, M. Creamer, M. Dotcheva, J. Radulovic, and J. Buick, *Int. J. Rotating Machinery* **2019** Article ID 7415263 (2019).
- [7] J. D. Jaramillo, B.S. Thesis, Houghton College, 2017.
- [8] D. J. Eager, B.S. Thesis, Houghton College, 2018.
- [9] J. S. Martin, B.S. Thesis, Houghton College, 2019.
- [10] J. G. Durbin, B.S. Thesis, Houghton College, 2019.
- [11] DOE Fundamentals Handbook: *Thermodynamics, Heat Transfer, and Fluid Flow* (Dept. of Energy, Washington D.C., 1992).
- [12] L. Euler, *Novi Commentarii academiae scientiarum Petropolitanae* **6**, 271-311 (1761).
- [13] "Principles of the Motion of Fluids" [Online]. The Euler Archive.
https://scholarlycommons.pacific.edu/euler-works/258/?utm_source=scholarlycommons.pacific.edu%2Feuler-works%2F258&utm_medium=PDF&utm_campaign=PDFCoverPages
- [14] J. B. Barlow, W. H. Rae, Jr, A. Pope, *Low-Speed Wind Tunnel Testing*, 3rd ed. (John Wiley & Sons, Inc., 1999).
- [15] F. T. Wattendorf, *Proceedings of the Fifth International Congress for Applied Mechanics*, (1939), pp. 526-530.
- [16] W. T. Eckert, K. W. Mort, and J. Jope, NASA TN D-8243 (1976).
- [17] M. Van Dyke, *An Album of Fluid Motion*, 1st ed. (The Parabolic Press, Stanford, 1982).
- [18] R. D. Blevins, *Applied Fluid Dynamics Handbook* (Van Nostrand Reinhold Co., New York, 1984).